CHAPTER III

RESULTS AND DISCUSSION

The goal of this research is to introduce charged functional groups to the surface of chitosan films. The first method involves the reaction between amino group ($-NH_2$) of chitosan with methyl iodide (MeI) to form positively-charged quaternary ammonium group. The second method is to attach a molecule containing a negatively-charged sulfonate group by the reaction between amino group and 5-formyl-2-furan sulfonic acid (FFSA) followed by reduction by $NaBH_4$. Adsorption of selected proteins having different molecular weight and charge characteristic on surface-modified chitosan films is determined. The correlation between the charge characteristic of surface-modified chitosan film and the charge of protein is addressed

3.1 Determination of % degree of deacetylation (%DD) of chitosan by ^1H NMR

Percentage of substitution of amino group of chitosan by charge functionality can be calculated from a number of amino groups available per chain of chitosan which is generally expressed as degree of deacetylation (%DD). %DD is defined as the percentage of glucosamine units in the chitosan chain and can be determined by NMR analysis. According to ^1H NMR spectrum of an original chitosan film shown in Figure 3.1, there is a broad signal at 3.4-3.8 ppm, assigned to $H_{2'}H_3$, H_4, H_5 and H_6, and a signal between 4.7 and 5.5 ppm, assigned to H_1 protons. The signal for H_2 is at 2.95 ppm. Integrations of methyl protons from *acetamides* ($-C\underline{H}_3$ of GlcNAc, δ 1.84 ppm) and proton ($-C\underline{H}NH_2$ of GlcN, δ 2.94 ppm) are shown in Table 3.1.

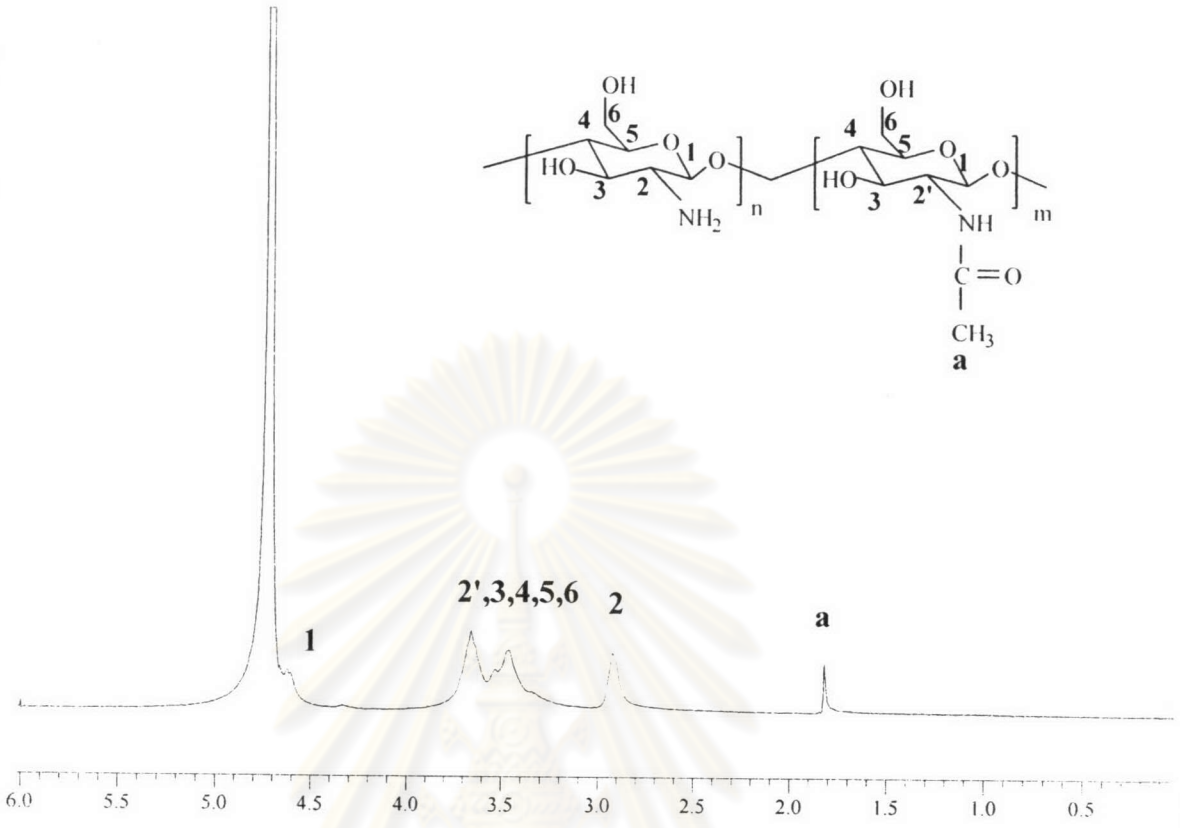

Figure 3.1 ^{1}H NMR spectrum of chitosan from Seafresh Chitosan (Lab) Co., Ltd. (solvent: 1% CF_3COOH in D_2O, 25 °C).

Table 3.1 Information from ^{1}H NMR spectrum of chitosan used in this study.

	δ (ppm)	**Integration**	**Relative Amount of units**
-C<u>H</u>NH_2 of GlcN	2.94	10	10/1
-C<u>H_3</u> of GlcNAc	1.82	4.2	4.2/3

Considering the total repeating units in chitosan as 100%, %DD of 87.72% was calculated based on the data in Table 3.1 using the following equation.

$$\%DD = \frac{\text{Amount of GlcN unit in chitosan}}{\text{The total amount of GlcN and GlcNAc units in chitosan}}$$

$$= \frac{(10/1)\times 100\%}{(4.2/3)+(10/1)} = 87.72\%$$

The methods for modifying the surface of chitosan film are outlined in Scheme 3.1 and 3.2. The first method involves the reaction between amino group ($-NH_2$) of chitosan with methyl iodide (MeI) to form positively-charged quaternary ammonium salts. The second method is to attach a molecule containing a negatively-charged sulfonate group by the reaction between the amino group of chitosan and 5-formyl-2-furan sulfonic acid (FFSA). Characterization of the modified chitosan films were carried out by means of NMR, ATR-IR, air-water contact angle measurement, XPS and zeta-potential.

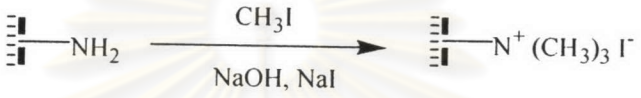

Scheme 3.1 Reaction between chitosan film and CH_3I.

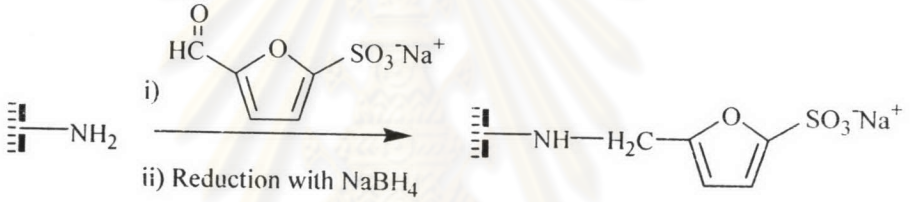

Scheme 3.2 Reaction between chitosan film and FFSA.

During the neutralization-drying steps (in NaOH-MeOH solution), the chitosan films swelled up and shrank, resulting in scattered wrinkle across the film piece. Only selected smooth areas of the films were, however, used for surface modification.

3.2 Preparation of positively-charged chitosan film

After quaternization reaction in alkaline condition, color of the resulting film was more yellowish, and its surface became less smooth than the original chitosan film. From ^1H NMR of chitosan film after quaternization illustrated in Figure 3.2, the signal at 3.2 ppm was assigned without ambiguity to the protons of three methyl groups of the quaternary ammonium salt. Other signals were assigned after examination of the 2D homonuclear ^1H-^1H correlation (Figure 3.3). The signals at 3.25, 2.90 and 2.65 ppm assigned to the trimethyl, dimethyl and methyl amino groups, respectively are not correlated with any chitosan protons. A weak peak at 3.35 ppm was assigned to methyl protons connected to oxygen (from hydroxyl group at 6^{th} position of chitosan) as a consequence of *O*–methylation. Similar peak assignments were previously reported by

others [11,29]. The fact that QAC formation can be demonstrated by a bulk characterization technique like NMR implies that the surface modification proceeded quite deep into the film.

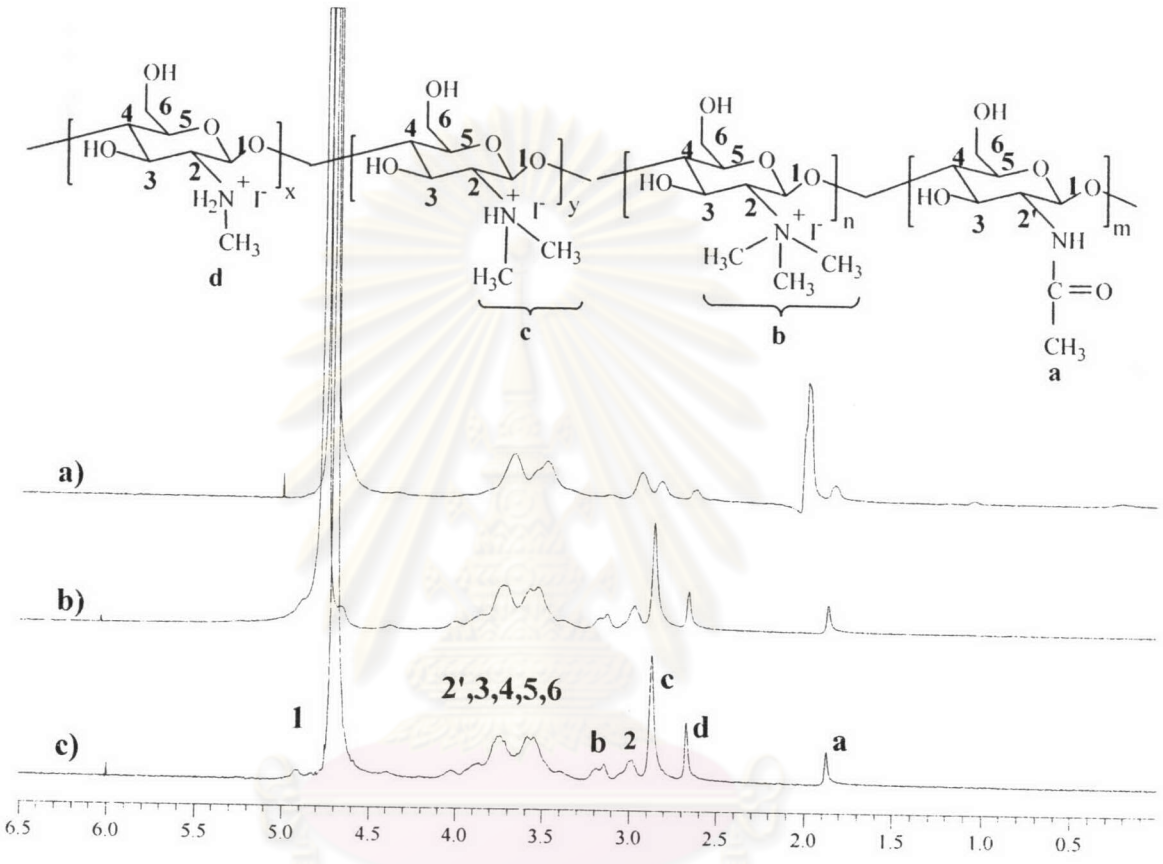

Figure 3.2 ^{1}H NMR spectrum of QAC-film reacted with (a)3 , (b)6 and(c) 12 equivalent of MeI (solvent: 1% CF_3COOH in D_2O, 25 °C).

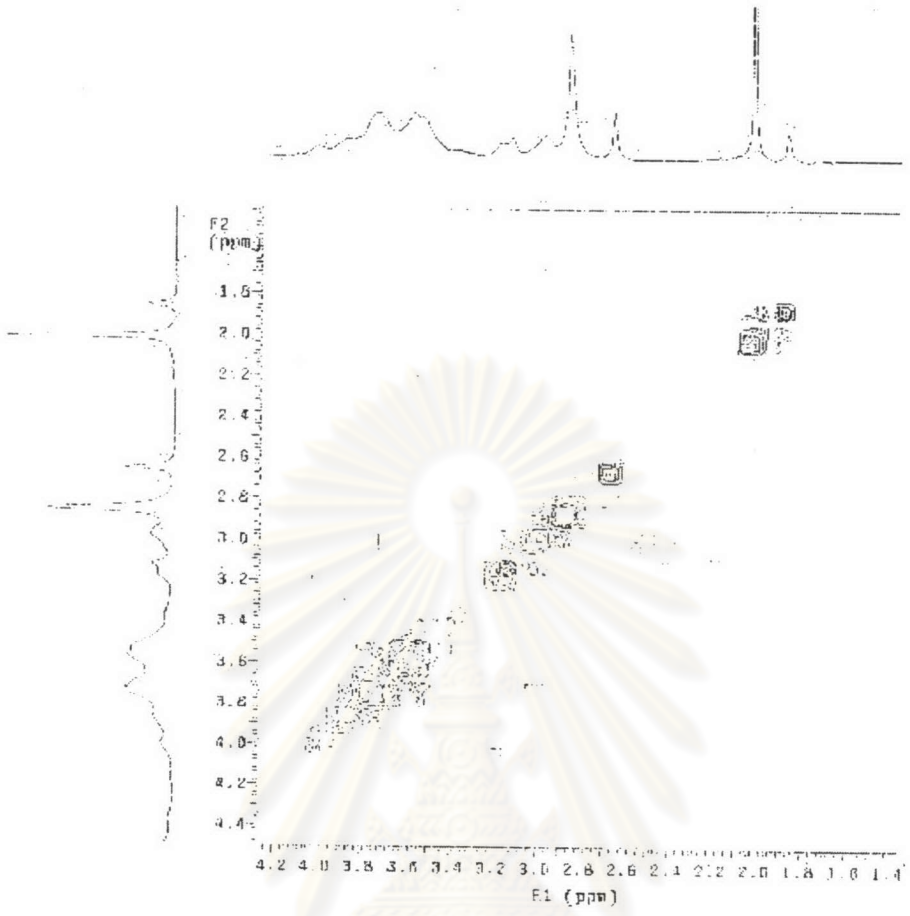

Figure 3.3 Contour plots from ^{1}H-^{1}H correlation of QAC film.

Table 3.2 Peak assignment for ^{1}H NMR spectrum of QAC film

Functional group	δ (ppm)
-NH–C<u>H</u>$_3$	2.65
-N(C<u>H</u>$_3$)$_2$	2.90
-N^{+}(C<u>H</u>$_3$)$_3$	3.25
-O-C<u>H</u>$_3$	3.35

Percentage of degree of substitution (%DS) of quaternary ammonium group can be determined from the relative ratio between the peak integration of 9 protons from 3 methyl groups of the quaternary ammonium salt with the peak integration of 5 protons of chitosan (δ 3.4- 3.8 ppm). Calculation based on the data in Table 3.3 using Equation 3.1 indicated that %DS was increased by increasing the mole equivalent of MeI in the

reaction. It should be noted that the calculated values are %DS of the whole film should presumably be lower than the actual %DS in the surface region.

$$\%DS = \{[CH_3]/ [H]x\ 5/9\} \times 100 \quad \text{..... (3.1)}$$

Table 3.3 Percentage of degree of substitution (%DS) of quaternary ammonium group on chitosan films after reacting with MeI in MeOH for 8 h as determined by ^{1}H-NMR

Equivalent of MeI	Integration		%DS.
	H-2,3,4,5,6 of chitosan	-C<u>H</u>$_3$ of -N$^+$(C<u>H</u>$_3$)$_3$	
3	10	0.1	0.5
6	10	0.7	3.9
12	10	0.9	5

Contact angle measurement was mainly used as a characterization tool to determine effects of experimental variables on the relative extent of charge formation. As reported by others [11-13], quaternary ammonium chitosan synthesized by homogeneous reaction showed higher solubility in water having a broader pH range in comparison with chitosan. So it was expected that surface hydrophilic of chitosan films should be increased after quaternization.

As mentioned earlier in the experimental section, the water contact angle was promptly measured within 5 seconds after water drop arrived at the film surface. The rapid measurement was necessary to assure that there was no error caused by water absorption of the film surface. The following paragraphs address the effects of reaction time and the amount of MeI on the extent of surface quaternization.

3.2.1. Effect of reaction time

The water contact angle data of QAC film shown in Figure 3.4 suggested that the surface of modified chitosan films became more hydrophilic after the quaternary ammonium groups were introduced. The contact angle has decreased from 79.6° for the unmodified film to its minimum of 63.2° after 8 h of reaction at 40 °C using 0.46 M MeI (3 equivalent) in MeOH.

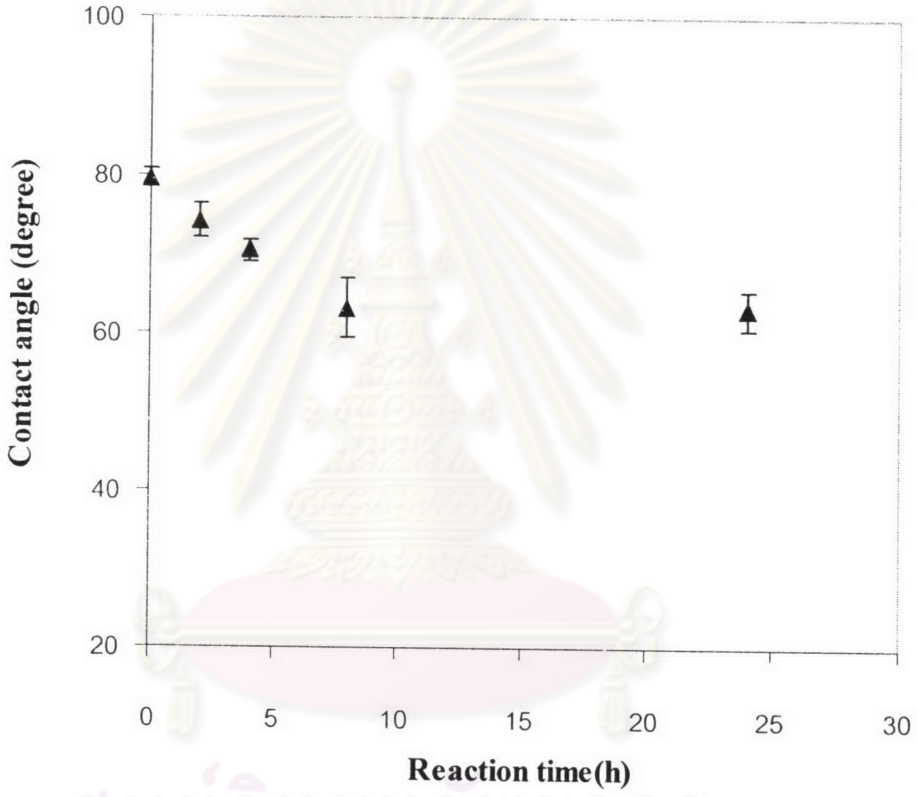

Figure 3.4 Correlation between air-water contact angle of QAC film and reaction time using 0.46 M MeI in MeOH at 40 °C. (n=5)

3.2.2 Effect of MeI:NH_2 ratio

As can be seen from Figure 3.5, the stoichiometric ratio of 3 for MeI: NH2 group of chitosan is enough to attain the maximum quaternization on the surface. An excess amount of MeI did not significantly increase the extent of reaction.

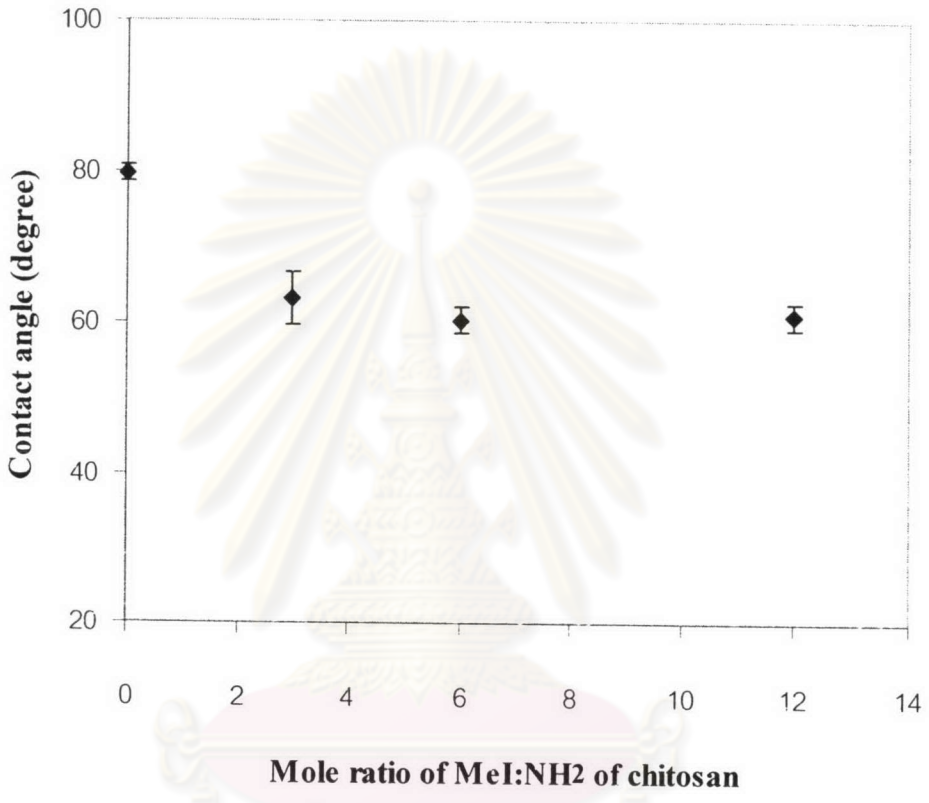

Figure 3.5 Correlation between air-water contact angle QAC film and MeI: NH_2 ratio using MeI in MeOH for 8 h. (n=5)

X-ray photoelectron spectroscopy was used to confirm the existence of quarternary ammonium group on QAC film. For the chitosan film (Figure 3.6), only signals from C_{1s} (285 eV), N_{1s} (402 eV) and O_{1s} (530 eV) of chitosan are visible. After the reaction with MeI (Figure 3.7), there were peaks appearing at ~619 eV and ~630 eV which were assigned to the I_{3d}, (a counter ion), verifying the presence of quaternary ammonium groups on the film. The absence of signal of I_{3d} on the unmodified chitosan surface (as a control surface) after exposure to NaI solution evidently suggested that the appearance of I_{3d} on the surface of QAC film was truly a consequence of ionic attraction between the quaternary ammonium group and iodide counter ion but was not caused by non-specific adsorption of iodide ion from NaI solution.

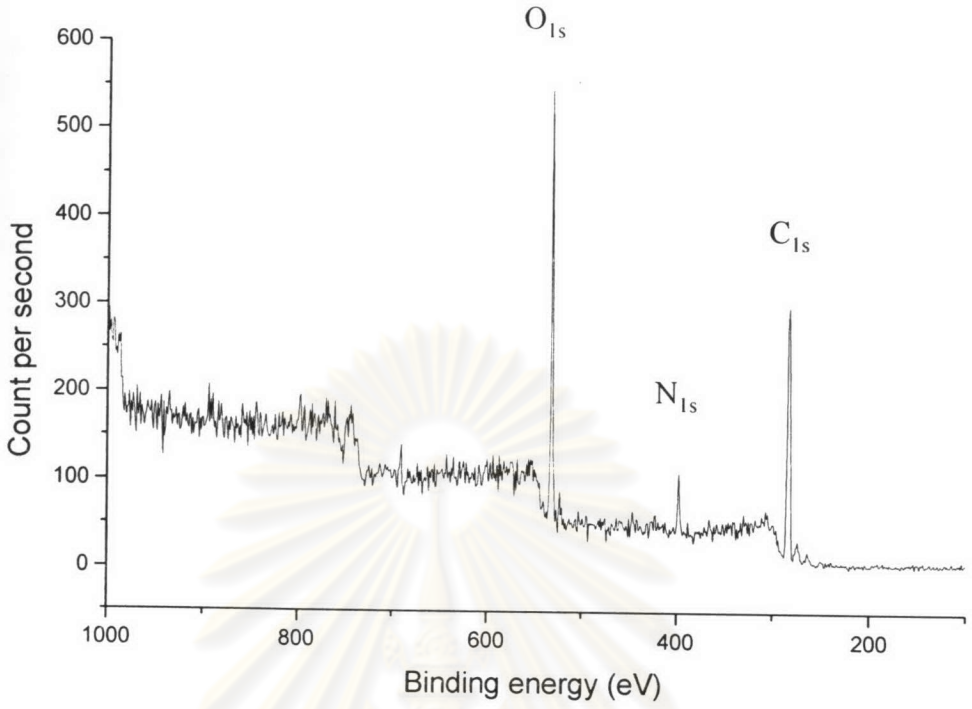

Figure 3.6 XPS survey spectrum of chitosan film.

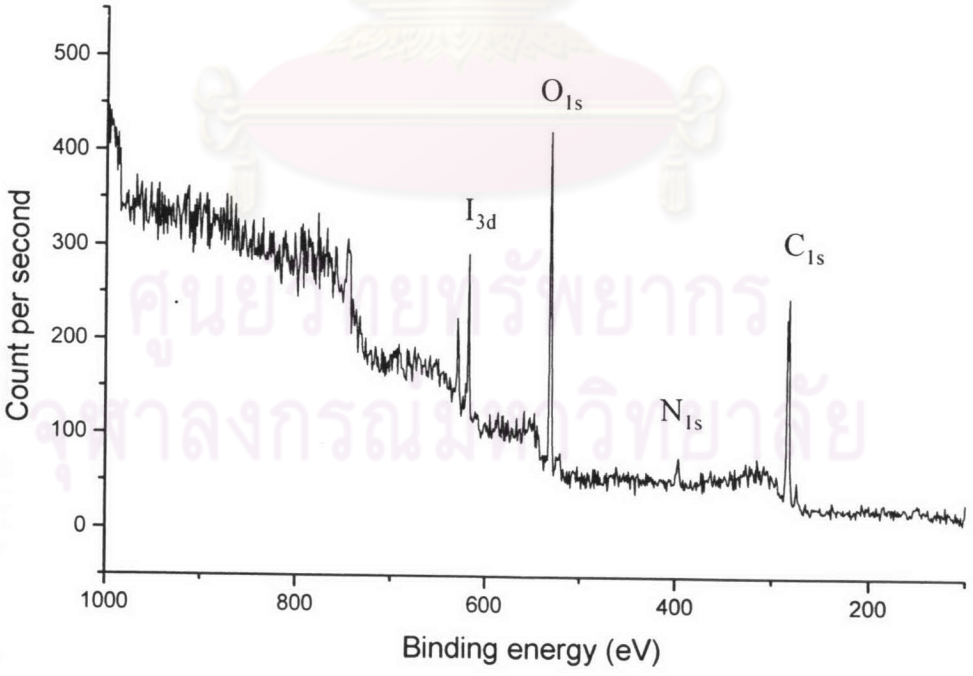

Figure 3.7 XPS survey spectrum of QAC-film.

Table 3.4 XPS atomic composition of chitosan and QAC films

Surface	Atomic compositon (%)			
	C	O	N	I
Chitosan	69.8	25.3	4.9	-
QAC-film	63.0	28.6	6.8	1.6

Table 3.4 lists XPS atomic composition of chitosan and a selected QAC film having the contact angle of 61.0±1.7. It was assumed that this surface-modified chitosan film contained the maximum density of quaternary ammonium group on the surface. Theoretically, there should be %I of approximately 1.6% if all amino groups of chitosan (based on %DD = 87.72%) are substituted by quaternary ammonium groups which bind stoichiometrically with iodide counter ions.

Taking the data in Table 3.4, %DD of 87.72%, %N of 4.9% and a = 1, %DS of 37.2% can be calculated using the equations shown below.

$$\frac{\%n}{\%N} = \frac{\%DD}{100} \qquad \text{.....(3.2)}$$

and

$$\%DS = \frac{(\%X/a)}{\%n} \times 100 \qquad \text{.....(3.3)}$$

%n is the percent mole of nitrogen of the amino groups in chitosan.

%N is the percent mole of nitrogen (both amino and amide groups) found on the film surface.

%X is the percent mole of halide atom found on the surface.

a is number of moles of halide atom in 1 mole of the compound.

Characterization of functional groups on the film surface before and after quaternization was performed by ATR-IR. In general, the sampling depth of ATR-IR is about 1-2 μm (deeper than XPS technique). Results are shown in Figure 3.8. Absorption peaks in Figure 3.8(a) at *ca.* 1650 and 1590 cm^{-1} were assigned to the carbonyl stretching of secondary amide (amide I) and N-H bending vibration (amide II) of the primary amine in glucosamine unit, respectively.

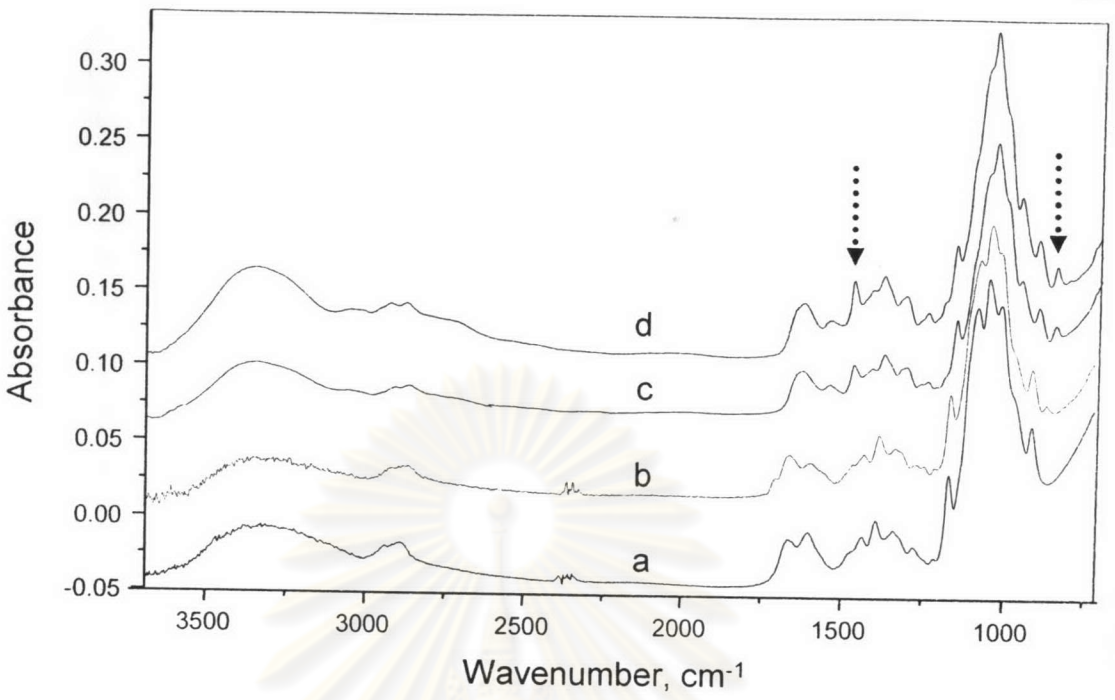

Figure 3.8 ATR-IR spectra of (a) chitosan film, QAC films as products of chitosan films reacted with (b) 3, (c) 6 and (d) 12 equivalent of MeI.

Figure 3.8 (b-d) shows ATR-IR spectra of QAC films prepared from chitosan films reacted with different equivalent of MeI. Upon increasing the amount of MeI, the intensity of the characteristic N-H bending peak of chitosan at 1590 cm^{-1} correspondingly decreased. The peaks at 1456 and 970 cm^{-1}, observed on the spectra of all QAC films are the characteristic peaks of the C-N stretching. The relative ratio of both C-N stretching signals increased with increasing equivalent of MeI in quaternization step, which helped promoting methylation of the amino groups.

3.3 Preparation of negatively-charged chitosan film

In this part, the negatively-charged chitosan film was prepared by means of attaching FFSA on the chitosan surface. Similar to the preparation of positively-charged chitosan film by surface quaternization, the preparation of negatively-charged chitosan by sulfonation was also carried out under heterogeneous condition. Since the sulfonation was conducted in MeOH which could be extensively absorbed by the chitosan films, the depth of surface modification was so great that the reaction can be monitored by ^1H NMR. Figure 3.9 shows ^1H NMR spectrum of

N-sulfofurfuryl chitosan prepared under heterogeneous condition (SFC film). The signals of two furan protons at 6.3 and 6.6 ppm evidently confirm the attachment of *N*-sulfofurfuryl moiety. Furthermore, there was a new signal appearing approximately at 4.4 ppm corresponding to the two protons of methylene groups that links between the amino group of chitosan and the furan ring. The analysis of the ^{1}H-^{1}H homonuclear correlation shown in Figure 3.10 also supports these assignments.

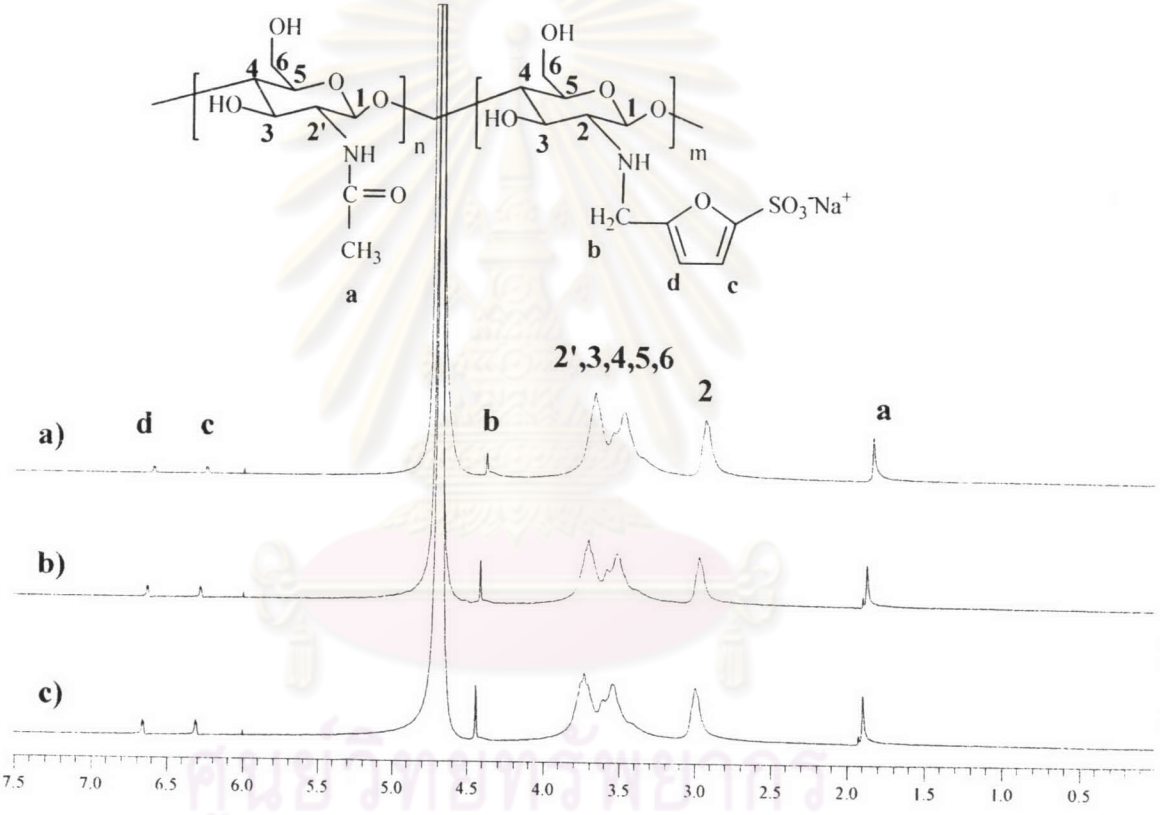

Figure 3.9 ^{1}H NMR spectrum of SFC film reacted with (a) 1, (b) 3 and (c) 5 equivalent of FFSA (solvent:1%CF_3COOH in D_2O, 25 ^{o}C).

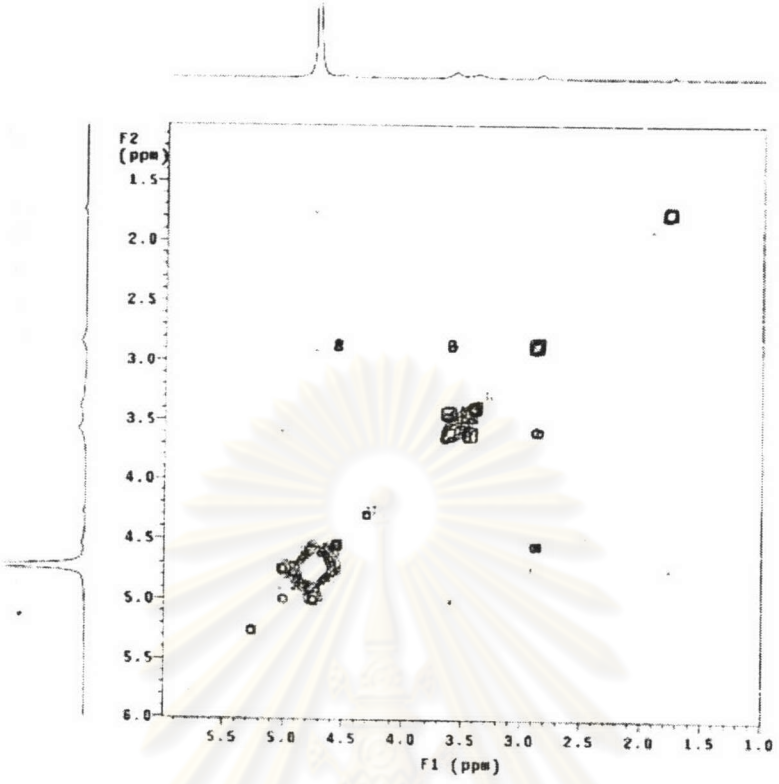

Figure 3.10 Contour plot from ^{1}H-^{1}H correlation of SFC film.

Table 3.5 Peak assignment for ^{1}H NMR spectrum for SFC film

Functional group	δ (ppm)
-NH–C$\underline{H_2}$ -	4.4
-HC=C$\underline{H}$-	6.6, 6.3

%DS of sulfonate group can be determined by the relative ratio between the peak integration of 2 protons of methylene group (-CH_2-) that links the amino group of chitosan to the furan ring of FFSA and the peak integration of the proton H_2 of chitosan. Using equation 3.4, %DS can be calculated and are shown in Table 3.6.

$$\%DS = \{[CH_2]/ [H]x\ 1/2\} \times 100 \qquad \text{..... (3.4)}$$

Table 3.6 Percentage of degree of substitution (%DS) of sulfonate group on chitosan films after reacting with FFSA in MeOH for 24 h as determined by ^{1}H-NMR.

Equivalent of FFSA	Integration		%DS.
	H-2 of chitosan	-C<u>H</u>$_2$ of - NC<u>H</u>$_2$-fur	
1	21.5	1.9	4.4
3	21.6	3.3	7.6
5	21.9	3.4	7.7

%DS of sulfonate group on chitosan film was apparently elevated from 4.4 to 7.7 when the chitosan/FFSA ratio was increased from 1:1 to 1:6. Once again, it should be noted that the calculated values are %DS of the whole film should presumably be lower than the actual %DS in the surface region. Air-water contact angle measurement was used as a tool to follow the extent of surface sulfonation as a function of reaction time and FFSA concentration based on the assumption that the higher content of sulfonate group, the lower the contact angle.

3.3.1 Effect of reaction time

The contact angle data shown in Figure 3.11 reveal that the longer the reaction proceeded, the more hydrophilic the surface became.

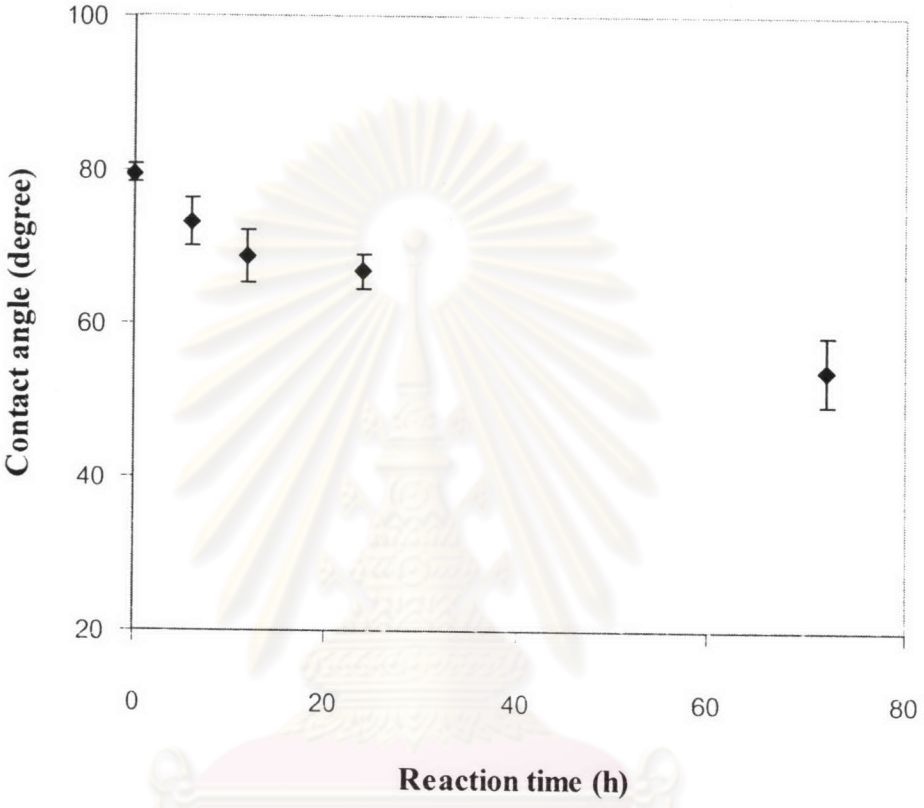

Figure 3.11 Correlation between air-water contact angle of SFC film and reaction time using 0.10 M FFSA in MeOH. (n=5)

3.3.2 Effect of FFSA: NH_2 ratio

Contact angle data of chitosan films after surface sulfonation illustrated in Figure 3.12 suggests that as high as 5 equivalents of FFSA (compare to -NH_2 groups) was necessary to achieve the maximum extent of reaction. This assumption agrees quite well with %DS previously estimated by ^{1}H NMR analysis.

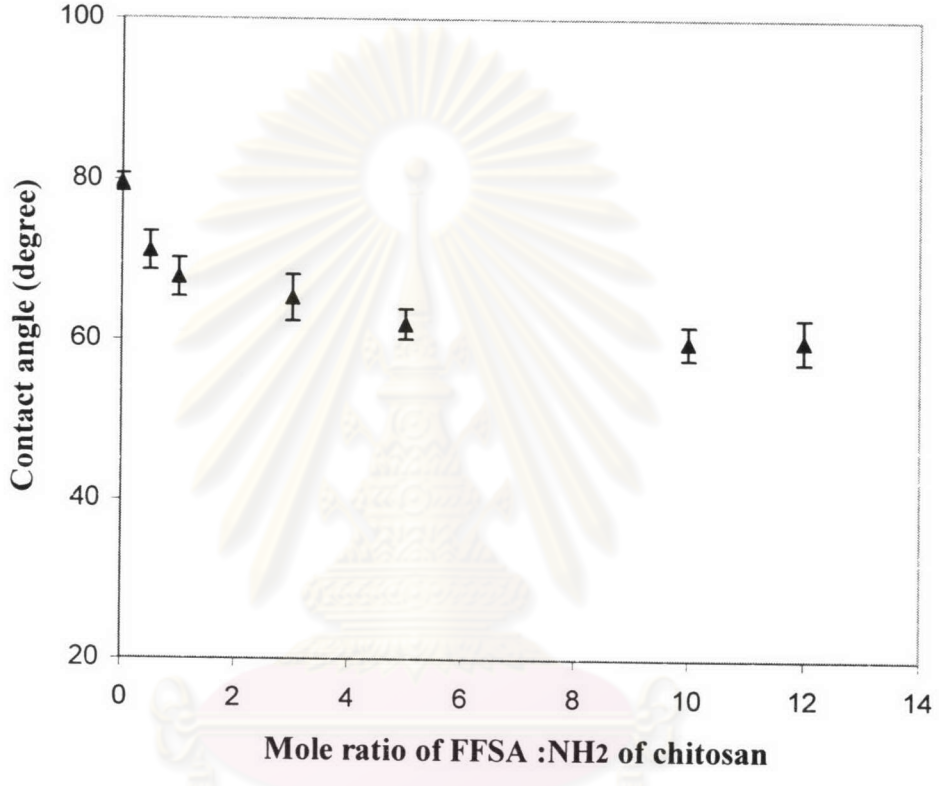

Figure 3.12 Correlation between air-water contact angle and FFSA: NH_2 ratio using FFSA in MeOH for 24 h. (n=5)

The XPS spectrum of a selected SFC film having contact angle of 62.0±1.9 is presented in Figure 3.13. It was assumed that this surface-modified chitosan film contained the maximum density of sulfonate group on the surface. The spectrum shows peaks representing carbon, oxygen, nitrogen and sulfur atoms. The appearance of the S_{2p} peak at 168 eV directly confirmed the substitution of FFSA. Moreover, this spectrum exhibited a peak of Na_{1s} at 1072 eV, indicating the existence of sodium as a counter ion for sulfonate group.

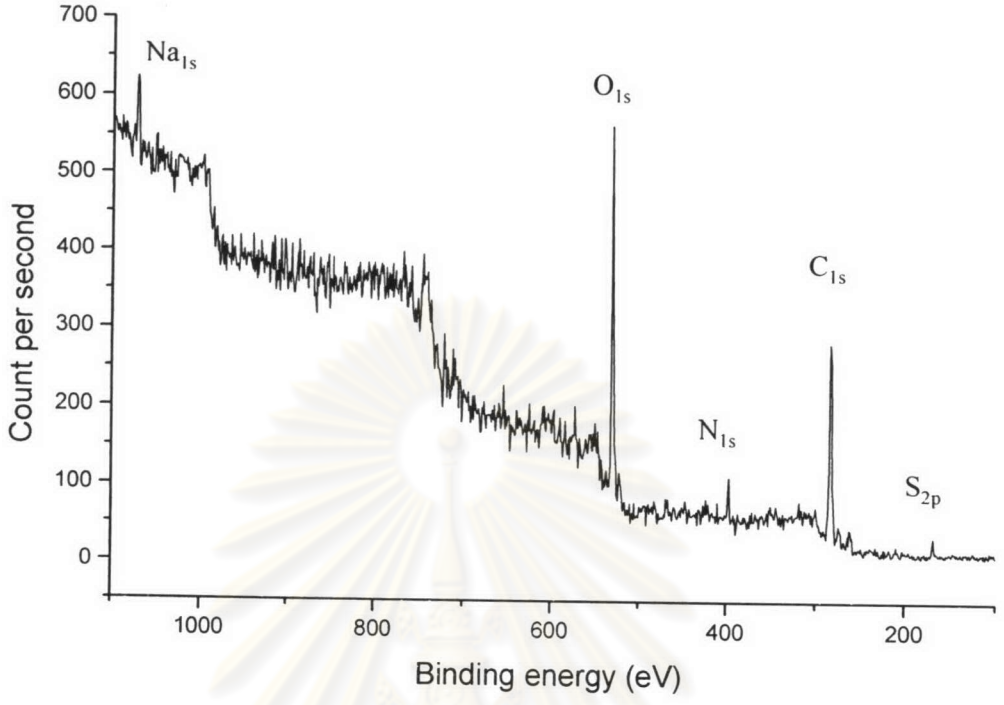

Figure 3.13 XPS survey spectrum of SFC film.

Table 3.7 XPS atomic composition of chitosan and SFC film

Surface	Atomic composition (%)				
	C	O	N	S	Na
Chitosan	69.8	25.3	4.9	-	-
SFC-film	62.2	29.9	4.9	0.9	2.1

Taking the data in Table 3.7, %DD of 87.72%, %S of 0.9%, %DS of 20.9% can be calculated using equations 3.2 and 3.3.

The ATR-IR spectra of SFC films prepared from different concentration of FFSA are shown in Figure 3.14. The presence of a signal from S=O stretching in the range of 1050-1200 cm^{-1} confirmed the success of surface sulfonation which have proceeded to the depth of at least 1-2 μm.

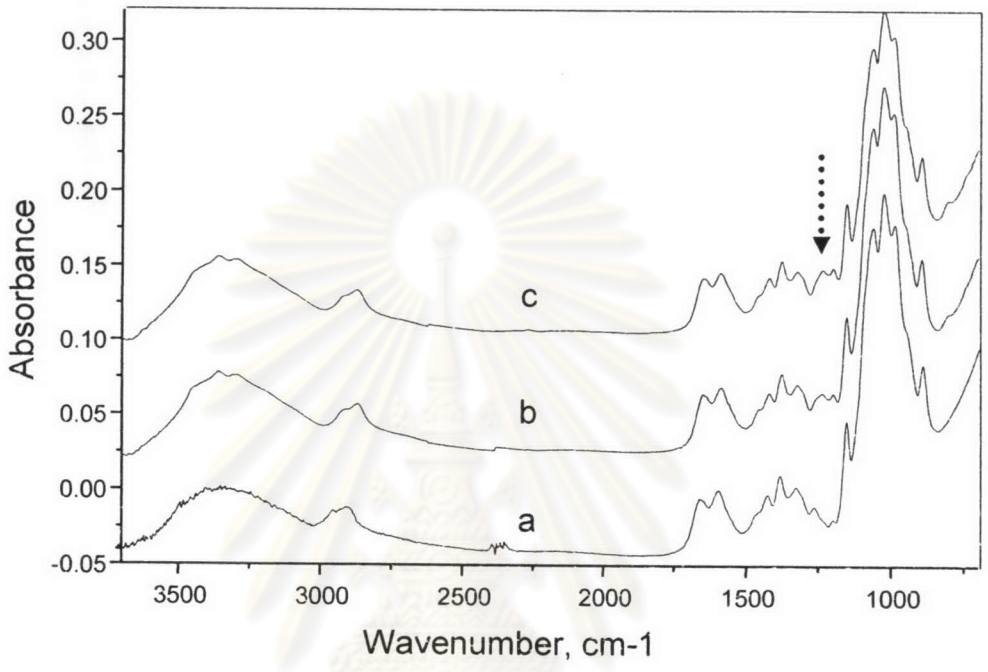

Figure 3.14 ATR-IR spectra of (a) chitosan film, SFC films as products of chitosan films reacted with (b) 1 and (c) 5 equivalent of FFSA.

3.4 Charge characteristic by zeta-potential measurement

Since the zeta potential can be related to the surface charge density, measurement of the zeta potential readily represents the electrostatic properties of the surface. The zeta potential was determined using distilled water as flow fluid. Results are shown in Figure 3.15. The QAC film has positive zeta potential whereas all SFC film exhibit negative values. In addition, the amount of negative charges on SFC film increased with increasing amounts of FFSA reagent from 0.5, 1 and 5 equivalents of the total amino groups in chitosan film. The zeta potential of neutral chitosan film however is found to be negative. No clear explanation for this unexpected charge characteristic can be made at this point. Nonetheless, Kato and coworkers have previously reported a negative value of zeta potential of -56.6 mV for a virgin PET fiber [23]. When the PET was grafted with anionic and cationic monomers; acrylic acid and dimethylamino ethyl methacrylate (DMAEMA), their zeta potentials were -35.3 and +66.2 mV, respectively.

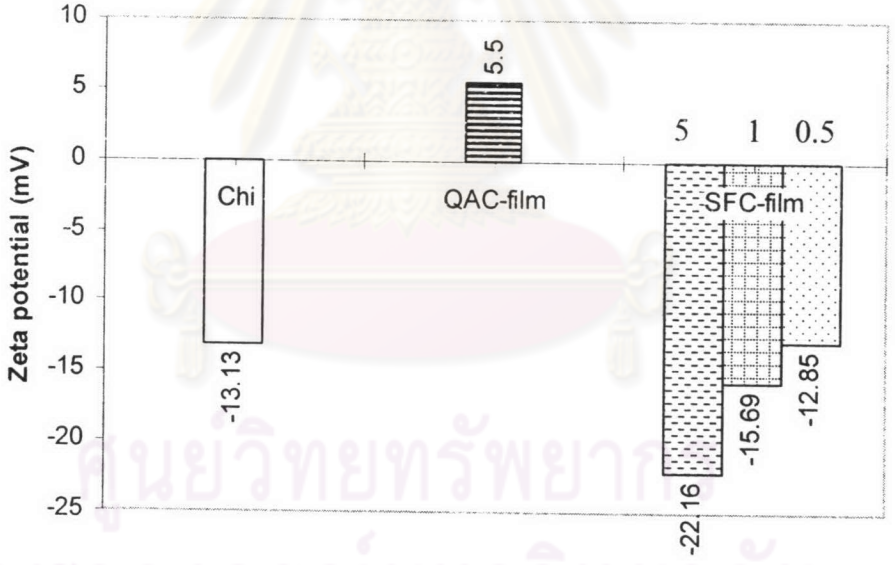

Figure 3.15 Zeta-potential data of unmodified and modified chitosan films.

3.5 Protein adsorption of surface-modified chitosan films

To address the hypothesis that charged surface can affect protein adsorption, adsorption of charged proteins on surface-modified chitosan films were investigated. The proteins used in this investigation include albumin, fibrinogen, lysozyme and ribonuclease (RNase) whose physical properties of these proteins are listed in Table 3.8. All proteins are globular proteins and vary in size, charge as well as conformational stability under the experimental condition (pH 7.4 buffers).

Table 3.8 Physical properties of proteins used in this investigation

	albumin	fibrinogen	lysozyme	RNase
Mass (Da)	69,000	34,000	14,600	13,680
Dimensions(nm)	$7 \times 4 \times 4$	$47 \times 5 \times 5$	$4 \times 3 \times 3$	$4 \times 3 \times 2$
Isoelectric point (pH units)	4.8	5.5	11.1	9.4
Diffusion coefficient ($m^2\ s^{-1}$)	7.4×10^{-11}	-	1.04×10^{-10}	1.26×10^{-11}

The amount of protein adsorption on the film surface was determined by bicinchoninic acid (BCA) assay. A calibration curve using albumin as a standard is displayed in Appendix B. The color intensity of protein solution after adding BCA working solution depends on the concentration of protein solution.

3.5.1 Adsorption isotherm

Adsorption isotherm is a relationship between the concentrations of adsorbate in solution and the surface coverage of the adsorbent at constant temperature Adsorption isotherms of all proteins were determined in order to seek for the adsorption capacity of a surface and the optimum concentration for comparative adsorption studies. The initial concentration of each protein was varied in the range of 0.1 - 2 mg/ml. The charged chitosan films used for these studies were the ones having the lowest contact angle values; 62.0±1.9 for QAC and 61.0±1.7 for SFC film.

Adsorption isotherms of albumin (BSA) on SFC, QAC and chitosan films are summarized in Figure 3.16. BSA adsorbed the least on the SFC film, followed by chitosan and QAC film, respectively. Similar to albumin, the fibrinogen (FIB) showed a greater adsorption capacity on QAC film than chitosan and SFC (Figure 3.17). Such a trend was governed by the electrostatic attraction and repulsion between the charged surface and the negatively-charged BSA and FIB. All isotherms showed that a concentration of 1 mg/ml of protein concentration is sufficient to reach the maximum adsorption capacity in all cases.

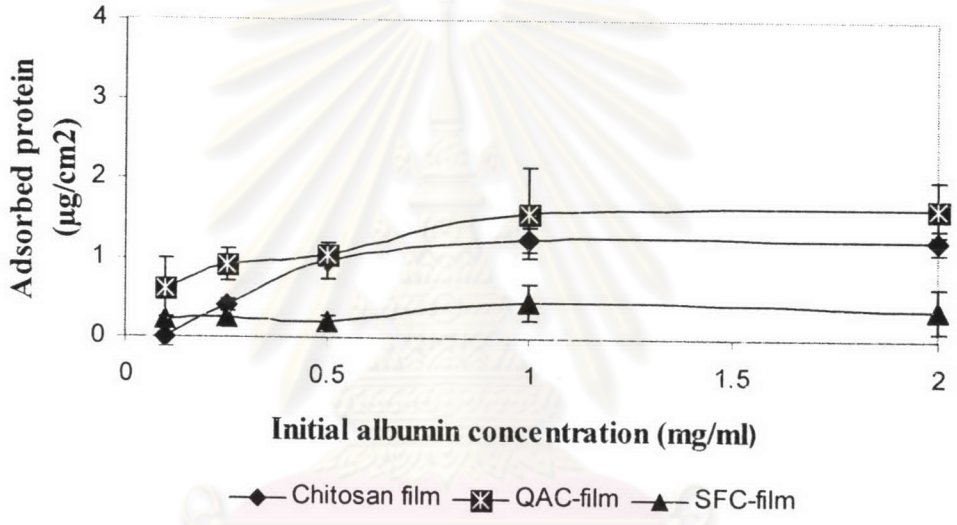

Figure 3.16 Adsorption isotherms of BSA on unmodified and modified chitosan films.

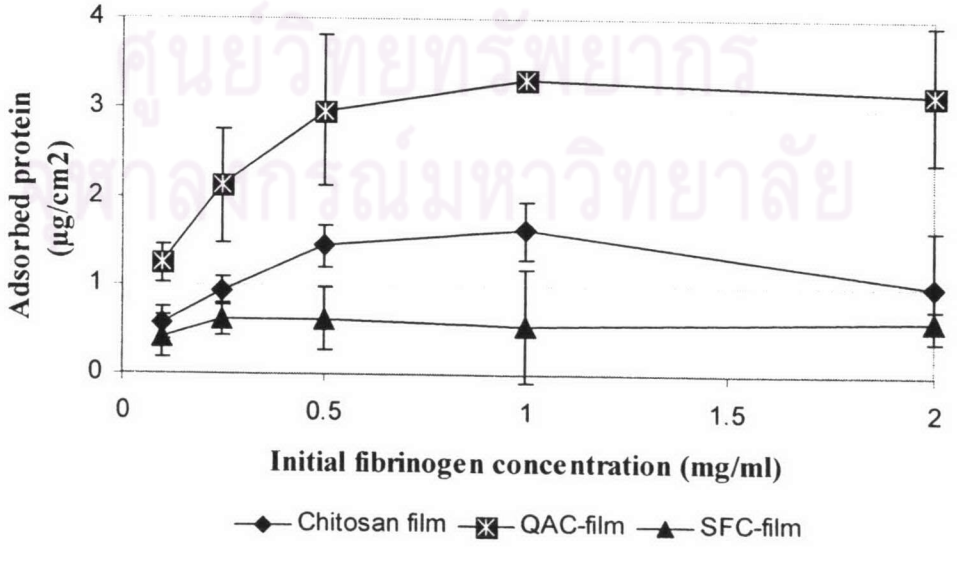

Figure 3.17 Adsorption isotherms of FIB on unmodified and modified chitosan films.

For lysozyme (LYZ) (Figure 3.18), an increase in the initial lysozyme concentration in the adsorption medium led to an increase in the amount of adsorbed LYZ on all tested samples. A concentration of 1 mg/ml was also a value that was on a plateau region of LYZ adsorption isotherm. The amount of LYZ adsorbed on positively-charged QAC film was unexpectedly higher than that adsorbed on SFC film. This outcome implied that protein adsorption may not only be influenced by the charge-charge interactions between the modified surface and proteins (attraction vs repulsion), but also by the size of protein. It was postulated that LYZ was readily absorbed into the bulk because of its small dimension and relatively high diffusion coefficient in comparison with other proteins especially in the case of highly swollen QAC film. The greater amount of adsorbed LYZ than other proteins on all tested substrates warranted the assumption that swelling played a significant part in protein adsorption. QAC was found to swell up to 153.3% after soaking in PBS at ambient temperature for 7 h, whereas SFC and chitosan films can swell up to 113.3% and 62.5%, respectively. This is the reason why the amount of adsorbed LYZ was very high despite the same charge between LYZ and the QAC film. In addition, the adsorption isotherm of LYZ on QAC film exhibited 2-step characteristic which may be an evidence indicating that the adsorbed layer was not monolayer. In addition to the swelling, the fact that LYZ can self-associate in solution, forming dimers and higher oligomers, particularly at pH 6-8 and high protein concentration may be another reason why the adsorbed amount of LYZ was so high and the adsorbed layer was not monolayer[30-32].

Adsorption isotherms of RNase are plotted in Figure 3.19. Unlike LYZ, an increase in the adsorbed amount of RNase on-each modified chitosan film follow an anticipated trend when the protein concentration was not higher than 0.5 mg/ml. As a consequence of negatively-charged RNase, its adsorption on QAC film was the least , followed by chitosan and SFC film, respectively. The amount of adsorbed RNase was however higher than those of other proteins when protein concentration was raised to 1 mg/ml. Even though RNase is a small protein, its diffusion coefficient is not quite high. This may be the reason why relatively high protein concentration (higher than 1 mg/ml) was required to drive. It was also believed that the adsorption isotherm is not Langmuir-type. Similar to LYZ, the 2-step adsorption characteristic caused the amount of adsorbed RNase to increase.

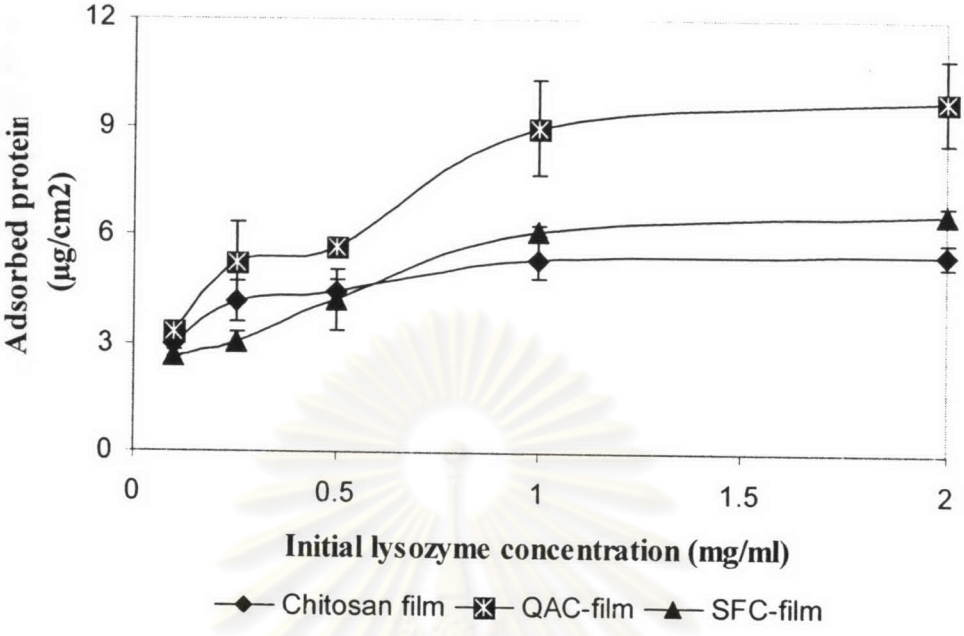

Figure 3.18 Adsorption isotherms of LYZ on unmodified and modified chitosan films.

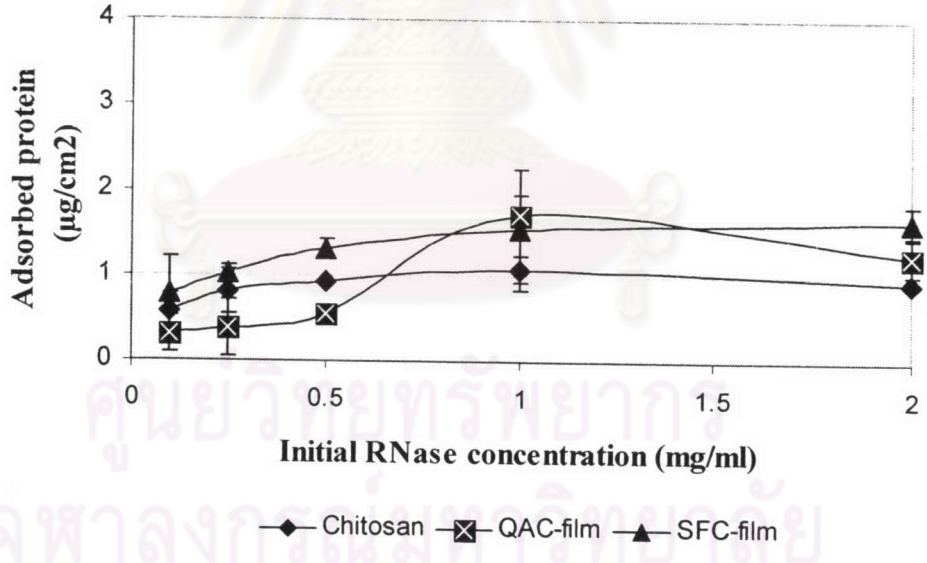

Figure 3.19 Adsorption isotherms of RNase on unmodified and modified chitosan films.

3.5.2 Effect of surface charge on protein adsorption

The adsorbed amounts at quasi-steady state with respect to adsorption isotherm plateau are plotted in Figure 3.20-3.23. The results demonstrate that the influences of the type and the amount of charge on protein adsorption appear to be substantial in all cases.

3.5.2.1 Albumin (BSA) and fibrinogen (FIB)

Albumin (BSA) and fibrinogen (FIB) were selected as models of negatively-charged proteins. Adsorbed amounts of BSA on SFC films having water contact angle of 71.2±2.6, 67.8±3.8 and 62.0±1.9, obtained from chitosan films reacted with 0.5, 1 and 5 equivalent of FFSA (compared to amino groups of chitosan), respectively are shown in Figure 3.20. Since the SFC film bears the same charge as BSA, electrostatic repulsion, therefore plays an important role in the adsorption. Increasing the equivalent of FFSA to react with chitosan film which corresponded with the charge density of sulfonate groups caused a reduction in BSA adsorption. For QAC film, the effect of electrostatic attraction became significant since BSA and surface carried opposite charges. Correspondingly, the strong electrostatic attraction renders the maximum adsorbed BSA on QAC film which was prepared from chitosan film reacted with MeI (12 eq.) for 8 h and had water contact angle of 61.0±1.7. The amount of adsorbed BSA also varied as a function of the equivalent of MeI. The more the MeI used, the higher the quantity of adsorbed BSA.

FIB is the largest protein studied (Table 3.8). Its isoelectric point is close to that of BSA; therefore it is also acidic protein that bears positive charges at this experimental pH. According to the results shown in Figure 3.21, the electrostatic interaction between FIB and the films was similar to that between BSA and the films. The electrostatic repulsion clearly decreases the amount of adsorbed FIB on SFC film having increasing charge density which was varied as a function of FFSA equivalent. From the electrostatic perspective, the higher adsorbed amount took place on QAC film having lower water contact angle obtained from the reaction that was carried out using more MeI mole ratio and longer reaction time.

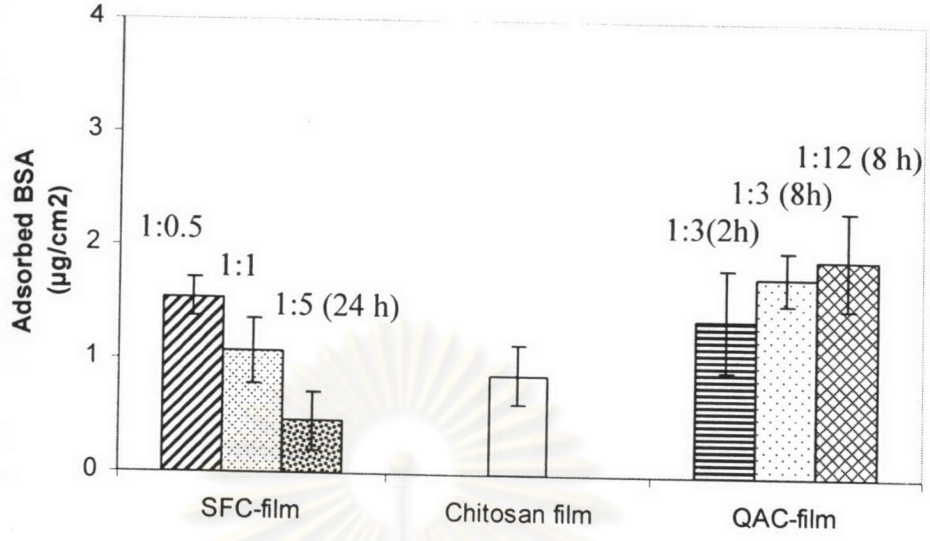

Figure 3.20 Comparison of BSA adsorption on unmodified and modified chitosan films.

The equivalent of reagents and reaction times are written above its corresponding bar.

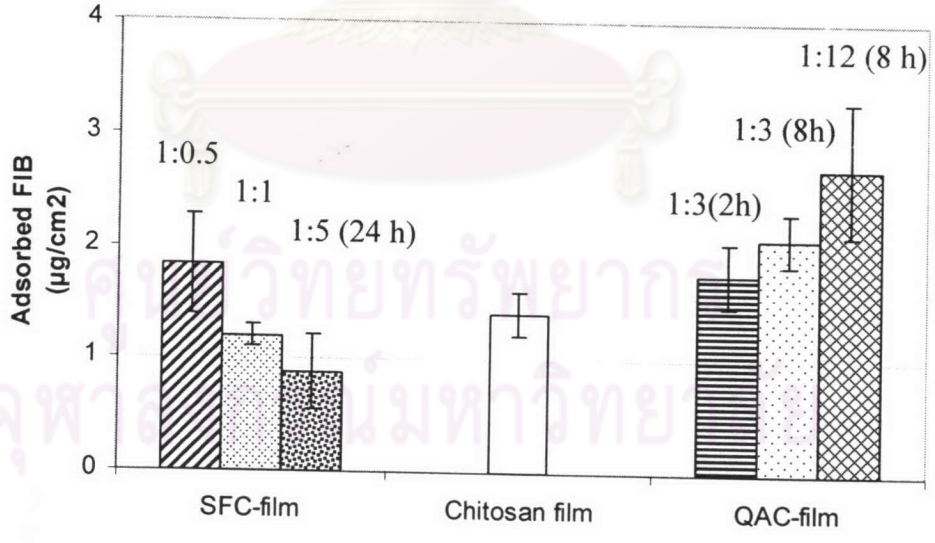

Figure 3.21 Comparison of FIB adsorption on unmodified and modified chitosan films.

3.5.2.2 Lysozyme (LYZ) and Ribonuclease (RNase)

Lysozyme (LYZ) and RNase are selected to be models for positively-charged proteins (Table 3.8). They both are small proteins considering only charge-charge interaction; the quantity of adsorbed protein should theoretically be more on SFC film than those on chitosan and QAC film. That was not the case, however. The proteins appeared to adsorb on the QAC film (Figure 3.22).

SFC films adsorbed larger amount of LYZ than chitosan film did. The amount of adsorbed LYZ on SFC film was inversely proportional to the charge density of the film which should be dependent on the water contact angle as well as the equivalent of FFSA used. The amount of protein adsorption was reduced as the higher equivalent of FFSA was used. It is possible that the adsorption of protein is not only driven by charge–charge attractive but also by hydrogen bonding. On the other hand, QAC films showed unusual trend of adsorption. There was more LYZ adsorbed on QAC film than those adsorbed on chitosan and SFC film. This implies that the unfavorable charge-charge repulsion between LYZ and the quaternary ammonium group on QAC film was outweighed by the swelling of film causing protein diffusion into the film. Air-water contact angles of all tested substrates are available in Table B-2, Appendix B.

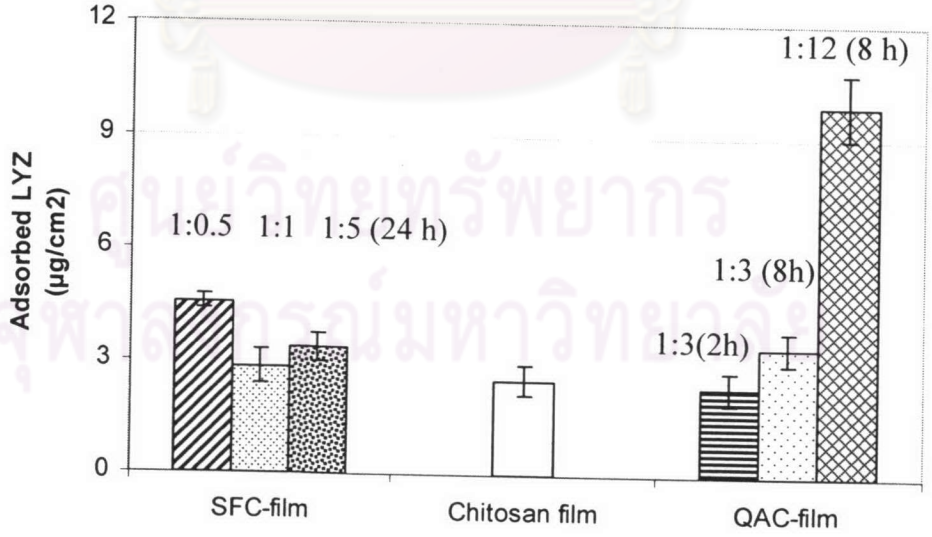

Figure 3.22 Comparison of LYZ adsorption on unmodified and modified chitosan films.

Ribonuclease (RNase), an enzyme which degrades RNA, is ubiquitous in living organisms and is exceptionally stable. As RNase carries a slight positive charge, electrostatic interaction was a driving force for adsorption on SFC film. Subsequently, adsorption was slightly improved on various SFC films when charged density increased. However, the adsorbed amount of RNase on SFC film was not significantly greater than that on chitosan film. For QAC film which carried the same charge as RNase, adsorption occurred independently on both charged surface and charged protein.

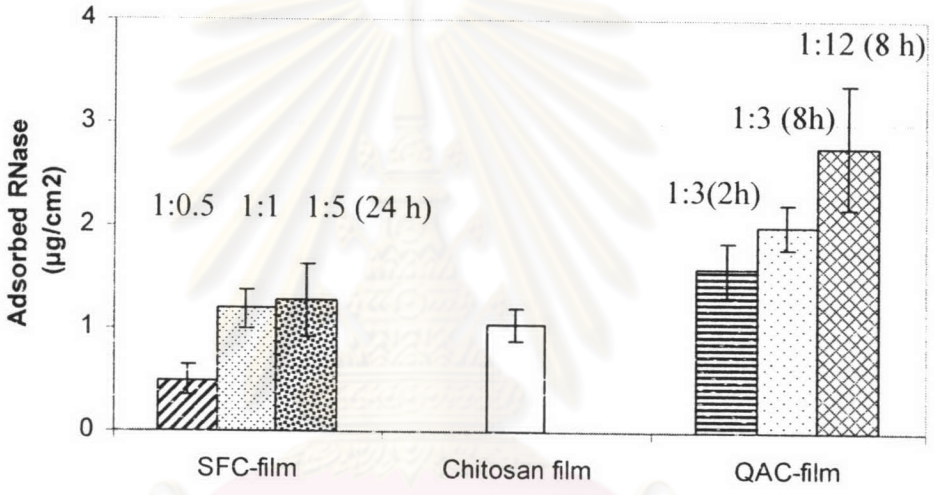

Figure 3.23 Comparison of RNase adsorption on unmodified and modified chitosan films.

According to a recent paper reported by Bos *et al.*, strong adsorption of positive charge LYZ and RNase on positively charged surface was obtained [33]. They used a semi conducting tin oxide layers substrate and varying surface charge by varying the applied interfacial potential. It was also found that at pH 9.9, more protein adsorbed as the surface–rendered more positive charges. The results obtained by Bos *et al.* are consequently in accordance with our results. On the contrary, another publication that was reported by Ladam *et al.* showed different trend [34]. LYZ and RNase adsorbed on positively charged PEI-$(PSS\text{-}PAH)_3$ less than the one adsorbed on a negatively-charged PEI-$(PSS\text{-}PAH)_3$ polyelectrolyte film due to electrostatic interaction. However, the reason of unusual results in this study is directed to the noticeable swelling of the QAC-film.

In comparison with others, the adsorbed amount per unit surface area obtained in this study is much greater than that on other types of surface. For example, Krisdhasima *et al.* [35] obtained a maximum adsorbed amount of 0.14 μg/ cm^2 for BSA on hydrophilic silica surfaces with a bulk concentration of 1 mg/ml at pH 7. However, the adsorbed amount obtained in this study is 1.91 μg/ cm^2 at the same pH value.